Journal of

Applied and Computational Mechanics

Shahid Chamran
University of Ahvaz

Investigation of Jeffery-Hamel Flow for Nanofluid in the Presence of Magnetic Field by a New Approach in the Optimal Homotopy Analysis Method

U. Biswal[1], S. Chakraverty[2]

[1] Department of Mathematics, National Institute of Technology Rourkela, Rourkela-769008, Odisha, India, Email: uddhababiswal789@gmail.com
[2] Department of Mathematics, National Institute of Technology Rourkela, Rourkela-769008, Odisha, India, Email: sne_chak@yahoo.com

Abstract. In this article, numerical study of nanofluid flow between two inclined planes is carried out under the influence of magnetic field. Water-based nanofluid with nanoparticle of Copper (Cu) is taken into consideration for the present investigation. An efficient numerical method namely Optimal Homotopy Analysis Method (OHAM) is employed to get an approximate series solution for the related governing differential equation. A new approach is proposed to determine the convergence controller parameters used in OHAM. For the validation of the proposed technique, the convergence of the obtained results is shown for different values of involved parameters. Moreover, residual errors for the different number of terms in the obtained series solution are represented graphically. Obtained numerical results from the proposed method are incorporated with the previous results and they are found to be in very good agreement. Impacts of involved parameters like nanoparticle volume fraction, Hartmann number and Reynolds number on non-dimensional velocity are also discussed.

Keywords: Jeffery-Hamel flow, Nanofluid, Numerical solution, Optimal Homotopy Analysis Method, Non-linear Ordinary Differential Equation.

1. Introduction

A fluid with suspended nanoparticles is known as nanofluid which is proposed by Choi [1]. These nanoparticles are generally made of carbide, nitride, metal, oxide, etc. Suspension of these nanoparticles in existing heat transfer fluids helps them to improve the thermal conductivity of the fluid. Because of higher thermal conductivity, nanofluid has more heat transfer capacity as compared to the traditional fluid. Due to its higher thermal conductivity, it has vast applications in the field of science and engineering such as heat exchangers, petroleum reservoirs, geothermal systems, etc.
From the last few years, nanofluid flow between plates is one of the important applicable cases in fluid dynamics. Few researchers have shown interested to study the fluid flow between two vertical planes and also between inclined planes. In order to investigate such problems, one may need to solve related governing differential equations analytically or numerically. But in most cases, related differential equations are highly non-linear so it may not be possible to get analytical solutions. As such related non-linear differential equations need to be handled numerically by efficient methods. Fluid flow due to the natural convection between two plates having different temperatures has been studied by a few authors [2-5]. Recently, incompressible fluid flow through a convergent-divergent channel is taken the attention of many researchers. Jeffery [6] and Hamel [7] were the first persons to investigate the fluid flow between two inclined planes and as a result, it's far referred to as Jeffery-Hamel problem. Jeffery-Hamel's problem has been studied extensively

by different researchers.

Esmaili et al. [8] have applied the Adomian Decomposition Method (ADM) to obtain an approximation to the analytical solution for the Jeffery-Hamel problem. ADM has been employed by Sheikholeslami et al. [9] to investigate the Jeffery-Hamel problem for nanofluid under the influence of high magnetic field. The effect of nanoparticles on Jeffery-Hamel flow has been discussed by Moradi et al. [10] for nanoparticles of alumina, titania, and copper. They have used the differential transformation method to handle the related non-linear differential equation. Umavathi and Shekar [11] have used the same method to observe the impact of the magnetic field on the Jeffery-Hamel flow for nanofluid. Homotopy Analysis Method has been used by Moghimi et al. [12] to handle the differential equation related to magneto-hydrodynamic (MHD) Jeffery-Hamel flow problem. Nourazar et al. [13] have used ADM to solve the governing equation for MHD Jeffery-Hamel flow of non-Newtonian Casson fluid in a stretching/shrinking convergent/divergent channel. Jeffery-Hamel problem has been investigated extensively by Turkyilmazoglu [14], where the walls of the stationary channels are permitted to stretch or shrink. Other numerical methods to handle the governing non-linear differential equation for fluid flow problems may also be found in [15-19]. Water-based nanofluids have been used by various authors to study nanofluid problems such as Turkyilmazoglu [20] has used water-based nanofluids to investigate the fully developed slip flow in concentric annuli via single and dual-phase nanofluid models. Turkyilmazoglu [21] has also used water-based nanofluid to study the cooling systems in Free and circular jets and noticed that the nanofluids indeed cool the system by increasing the nanoparticle volume fraction. Alsabery et al. [22] have used water-based nanofluids to study the natural convection of a nanofluid in an inclined square enclosure consisting of a porous layer and nanofluid layer. Boundary layer flow of nanofluids has been discussed by Turkyilmazoglu [23], where he has used water-based nanofluid with nanoparticles of Copper, Copper Oxide, Silver, Alumina and Titanium oxide.

Liao [24-25] has proposed a new approximation technique namely Homotopy Analysis Method (HAM) based on homotopy in topology in order to handle non-linear differential equations. The main merit of the homotopy analysis method is that its validity does not depend upon any small/large parameter involved in the non-linear differential equation. A generalized version of HAM known as OHAM is discussed in [26] which contains more than one convergence controller parameters. In this article, a new approach is used to get numerical values of the convergence controller parameters used in OHAM. Further, it is shown that the residual error tends to zero by taking more number of terms in the series solution.

2. Formulation of Problem

Let us consider the flow of nanofluid from a source or sink at a channel constructed by two rigid walls which are inclined at an angle of 2α as presented in Fig.1. The considered channel is said to be convergent or divergent accordingly as $\alpha < 0$ or $\alpha > 0$. It is considered that a magnetic field B_0 acts transversely to the fluid flow. For the present problem, we have assumed that the velocity is purely radial which depends only on r and θ such that $v = (u(r,\theta),0)$. It is also assumed that there is no magnetic field in the z-direction. The continuity, Navier-Stokes and Maxwell's equations in polar co-ordinates may be written as [11]:

$$\frac{\rho_{nf}}{r}\frac{\partial}{\partial r}\big(ru(r,\theta)\big) = 0, \tag{1}$$

$$u(r,\theta)\frac{\partial}{\partial r}\big(ru(r,\theta)\big) = \frac{-1}{\rho_{nf}}\frac{\partial P}{\partial r} + \frac{\mu_{nf}}{\rho_{nf}}\left(\frac{\partial^2}{\partial r^2}(u(r,\theta)) + \frac{1}{r}\frac{\partial}{\partial r}(u(r,\theta)) + \frac{1}{r^2}\frac{\partial^2}{\partial\theta^2}(u(r,\theta)) - \frac{u(r,\theta)}{r^2}\right) - \frac{\sigma B_0^2}{\rho_{nf}r^2}u(r,\theta), \tag{2}$$

$$\frac{1}{r\rho_{nf}}\frac{\partial P}{\partial\theta} - \frac{2}{r^2}\frac{\mu_{nf}}{\rho_{nf}}\frac{\partial}{\partial\theta}\big(u(r,\theta)\big) = 0 \tag{3}$$

Here $u(r,\theta)$ is radial velocity, P is the fluid pressure, B_0 stands for electromagnetic induction, σ denotes conductivity of the fluid, ρ_{nf} and μ_{nf} stand for effective density and effective dynamic viscosity of nanofluid respectively. The parameters ρ_{nf} and μ_{nf} may be expressed as [5,27,28]:

$$\rho_{nf} = \rho_f(1-\phi) + \rho_s\phi, \tag{4}$$
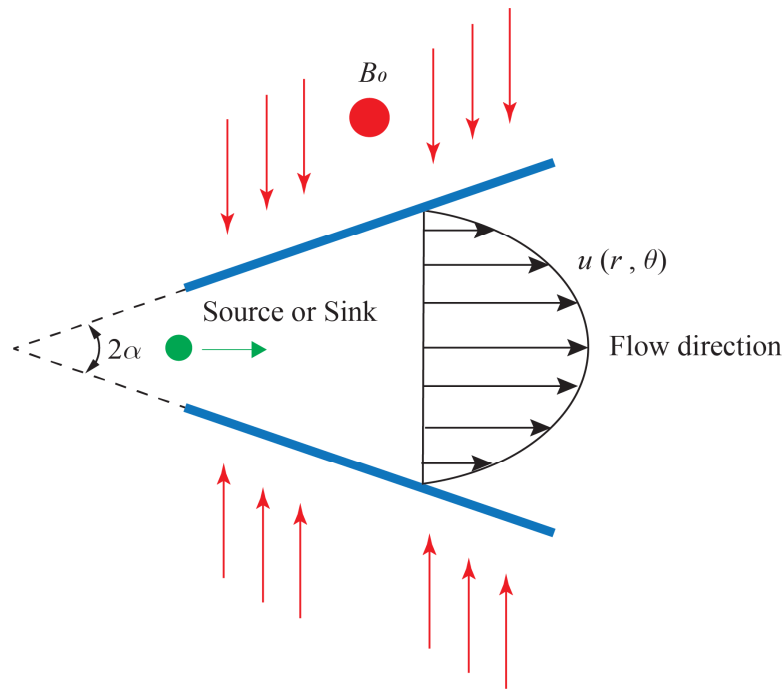
$$\mu_{nf} = \frac{\mu_f}{(1-\phi)^{2.5}} \tag{5}$$

Fig 1. Graphical representation of the problem.

Here ϕ denotes nanoparticle volume fraction. The boundary conditions are given as: $\partial u(r,\theta)/\partial\theta = 0$ at the center and $u(r,\theta) = 0$ at the boundary of the channel. Considering only radial flow, from the continuity equation we may obtain:

$$ru(r,\theta) = f(\theta) \Rightarrow u(r,\theta) = \frac{f(\theta)}{r} \tag{6}$$

In order to non-dimensionalize the governing differential equation, let us introduce dimensionless parameters as $\eta = \theta/\alpha$ for dimensionless degree and $F(\eta) = f(\theta)/f_{max}$ for dimensionless velocity parameter. Now by eliminating pressure term from Eqs. (2) and (3) and with the help of Eqs. (4) - (6) and defined dimensionless parameters, the dimensionless governing differential equation may be obtained as:

$$F'''(\eta) + 2\alpha.Re.A.(1-\phi)^{2.5}F(\eta)F'(\eta) + \left(4 - (1-\phi)^{2.5}(Ha)^2\right)\alpha^2 F'(\eta) = 0 \tag{7}$$

where Re denotes Reynolds number, Ha stands for Hartmann number which controls magnetic effect and A is the ratio of effective density of nanofluid and density of the base fluid. These parameters are expressed as:

$$Re = \frac{f_{max}\rho_f\,\alpha}{\mu_f} = \frac{U_{max}r\rho_f\,\alpha}{\mu_f}, \quad (Ha)^2 = \frac{\sigma B_0^2}{\mu_f} \quad \text{and} \quad A = \frac{\rho_{nf}}{\rho_f} = (1-\phi) + \frac{\rho_s}{\rho_f}\phi \tag{8a}$$

and the boundary conditions may be reduced to:

$$F(0) = 1, F'(0) = 0, F(1) = 0 \tag{8b}$$

The boundary condition $F(1) = 0$ indicates that the no-slip condition holds at the wall. Moreover, from $F(0) = 1, F'(0) = 0$, it may be observed that the dimensionless velocity has a maximum value at the centerline of the channel and hence its derivative is zero at the centerline. Some thermophysical properties of nanofluid used in further discussion are given in Table 1 [11, 28].

Table 1. Thermophysical properties of water and nanoparticles of copper.

Property	Pure water	Copper
$\rho(kg/m^2)$	997.1	8933
$\mu(Nm/s)$	1×10^{-3}	-

3. Methodology

In order to express the basic concept of OHAM for handling nonlinear ordinary differential equation, let us consider the nonlinear differential equation:

$$L(u(x)) + N(u(x)) + g(x) = 0$$

$$B(u(x)) = 0 , \quad x \in \Omega .$$

$$(9)$$

where L and N denote linear and nonlinear parts of the differential equation respectively. Here x is the independent variable, $u(x)$ is an unknown function, $g(x)$ is a known analytic function and B is a boundary operator. From Liao [26], in a generalized version of HAM known as OHAM the zeroth-order deformation equation is given as:

$$[1 - A_1(p)] L[\varphi(x,p) - u_0(x)] = h A_2(p) [L(\varphi(x,p)) + N(\varphi(x,p)) + g(x)] \tag{10}$$

where $u_0(x)$ is an initial approximation of $u(x)$ satisfying the given boundary condition, p is an embedding parameter lies in $[0, 1]$ and $A_1(p)$ and $A_2(p)$ are analytic functions satisfying $A_1(0) = A_2(0) = 0$ and $A_1(1) = A_2(1) = 0$. Clearly p is nothing but a special case of $A_1(p)$ and $A_2(p)$. As such the zeroth-order deformation in HAM is a special case of Eq. (10), where $A_1(p) = A_2(p) = p$. Moreover, the homotopy perturbation method (HPM) is a special case of Eq. (10), where $A_1(p) = A_2(p) = p$ and convergence controller parameter $h = -1$. In this method, by following Marinca et al. [29-30], we have considered $A_1(p) = p$ and $h A_2(p) = H(p)$ in eq. (10). As such zeroth-order deformation may be written as:

$$[1 - p] L[\varphi(x,p) - u_0(x)] = H(p) [L(\varphi(x,p)) + N(\varphi(x,p)) + g(x)] \tag{11}$$

Here $H(p)$ is called convergence controller function satisfying $H(0) = 0$ and $H(1) \neq 0$. By putting $p = 0$ and $p = 1$ in eq. (11), we will get $\varphi(x,0) = u_0(x)$ and $\varphi(x,1) = u(x)$ respectively. It may be worth mentioning here that when p varies from zero to one the solution $\varphi(x,p)$ varies from $u_0(x)$ to the solution $u(x)$. Now expand $\varphi(x,p)$ and $H(p)$ in Maclaurin's series of p as:

$$\varphi(x,p) = \sum_{n=0}^{\infty} u_n(x) p^n \text{ and } H(p) = \sum_{k=1}^{\infty} c_k p^k \tag{12}$$

Assuming that these two series in eq. (12) are convergent at $p = 1$, we may have the solution:

$$u(x) = \varphi(x,1) = \sum_{n=0}^{\infty} u_n(x) = u_0(x) + \sum_{n=1}^{\infty} u_n(x) \tag{13}$$

According to Liao [24], by plugging eq. (12) in eq. (11) and equating coefficients of p^n from both sides of the resulting equation we will get n^{th} order deformation. Now by solving the differential equations obtained in n^{th} $(n = 0, 1, 2, 3...)$ order deformation with appropriate boundary conditions, we may get $u_0(x)$ and u_n as a function of $x, c_1, c_2, c_3, ..., c_n$ i.e. $u_n(x, c_1, c_2, c_3, ..., c_n)$.

As such the nth order approximate solution of Eq. (9) may be expressed as:

$$\tilde{u}_n = u_0(x) + \sum_{m=1}^{n} u_m(x, c_1, c_2, ..., c_m) \tag{14}$$

Here it may be noted that the nth order approximate solution depends upon the convergence controller parameter vector $\bar{c}_n = (c_1, c_2, c_3, ..., c_n)$. It is worth mentioning here that eq. (14) is an approximate solution of Eq. (9), so when we substitute this solution in eq. (9) an error known as the residual error will exist that is: $R_n = L(\tilde{u}_n) + N(\tilde{u}_n) + g(x) \neq 0$ for n^{th} order approximation.

Now the continuous summation of the squared residual for n^{th} order approximation over the given domain may be expressed as:

$$S_n(\bar{c}_n) = \int_{\Omega} \{R_n\}^2 dx = \int_{\Omega} \{L(\tilde{u}_n) + N(\tilde{u}_n) + g(x)\}^2 dx , \quad n = 1, 2, 3, ... \tag{15}$$

Marinca et al. [29-30] have determined the optimal points $c_1, c_2, c_3, ..., c_n$ by minimizing the square residual error in eq. (15) for the nth order approximation such that:

$$\frac{\partial S_n\left(c_1, c_2, c_3, \ldots, c_n\right)}{\partial c_i} = 0, \quad i = 1, 2, 3, \ldots \tag{16}$$

Here we need to solve n coupled algebraic equations to get the optimal points $c_1, c_2, c_3, \ldots, c_n$. As such by increasing the number of terms, we have to solve more numbers of nonlinear coupled algebraic equations. For large n it will become more and more difficult and will be time-consuming to solve for $c_1, c_2, c_3, \ldots, c_n$.

3.1 Finding of Convergence Controller Parameters

To overcome the above disadvantage, let us minimize the square residual error at each order of approximation to calculate convergence controller parameters one at a time. As such, we need to solve one algebraic equation at n^{th} order approximation for the convergence controller parameter c_n.

The procedure to calculate the values of convergence controller parameters is by following the least square technique [31-32].

For 1st order approximation, square residual error R_1 contains only one convergence controller parameter c_1. As such for the optimal value of c_1, let us apply the least square technique to minimize the continuous summation of the squared residual error S_1 that is:

$$\frac{dS_1}{dc_1} = 0 \Rightarrow \frac{d}{dc_1} \int_\Omega \{R_1\}^2 \, dx = \int_\Omega 2R_1 \cdot \frac{dR_1}{dc_1} \, dx = 0$$
$$\Rightarrow \int_\Omega R_1 \cdot \frac{dR_1}{dc_1} \, dx = 0. \tag{17}$$

The optimal value c_1 may be obtained from the algebraic eq. (17). Further in 2nd order approximation, R_2 contains both c_1 and c_2. But from the previous step, we already have the optimal value c_1. As such by following the previous step, the optimal value of c_2 may be found from the algebraic equation:

$$\frac{dS_2}{dc_2} = 0 \Rightarrow \int_\Omega R_2 \cdot \frac{dR_2}{dc_2} \, dx = 0. \tag{18}$$

By proceeding like this, at the nth order approximation S_n consists of only one unknown parameter c_n whose optimal value can be determined directly from the algebraic equation:

$$\frac{dS_n}{dc_n} = 0 \Rightarrow \int_\Omega R_n \cdot \frac{dR_n}{dc_n} \, dx = 0. \tag{19}$$

Now by plugging the optimal values of convergence controller parameters in eq. (14), we may get the nth order approximation solution of eq. (9).

4. Application to the Present Problem

For simplicity, let us consider the notations $a = 2\alpha . Re. A.(1-\varphi)^{2.5}$ and $b = (4-(1-\varphi)^{2.5} Ha^2)\alpha^2$ in eq. (7). Now eq. (7) can be written as:

$$F'''(\eta) + a.F(\eta)F'(\eta) + b.F'(\eta) = 0 \tag{20}$$

Now we apply the above discussed method to solve eq. (20). By considering the linear operator as $F'''(\eta)$, zeroth-order deformation for eq. (20) may be constructed as:

$$(1-p)F'''(\eta) = H(p)\left[F'''(\eta) + aF(\eta)F'(\eta) + bF'(\eta)\right] \tag{21}$$

The next step is to substitute the convergence controller function $H(p) = \sum_{k=1}^{\infty} c_k p^k$ and assumed the series solution $F(\eta, p) = \sum_{n=0}^{\infty} F_n(\eta)p^n$ in eq. (21).

$$(1-p)\sum_{n=0}^{\infty} F_n''(\eta)p^n = \left(\sum_{k=1}^{\infty} c_k p^k\right)\left\{\sum_{n=0}^{\infty} F_n''(\eta)p^n + a\sum_{n=0}^{\infty} F_n(\eta)p^n \sum_{n=0}^{\infty} F_n'(\eta)p^n + b\sum_{n=0}^{\infty} F_n'(\eta)p^n\right\} \tag{22}$$

$$\Rightarrow (1-p)\left\{F_0'''(\eta) + F_1'''(\eta)p + F_2'''(\eta)p^2 + ...\right\}$$
$$= \left(c_1 p + c_2 p^2 + c_3 p^3 + ...\right)\Big[\left\{F_0''(\eta) + F_1'''(\eta)p + F_2''(\eta)p^2 + ...\right\}$$
$$+ a\left\{F_0(\eta) + F_1(\eta)p + F_2(\eta)p^2 + ...\right\}\left\{F_0'(\eta) + F_1'(\eta)p + F_2'(\eta)p^2 + ...\right\}$$
$$+ b\left\{F_0'(\eta) + F_1'(\eta)p + F_2'(\eta)p^2 + ...\right\}\Big]$$

Equating coefficient of the same power of p from both sides of eq. (22), we may obtain:

$$p^0 : F_0''' = 0 \tag{23}$$

and the boundary conditions will be:

$$F_0(0) = 1, \ F_0'(0) = 0, F_0(1) = 0 \tag{24}$$

$$p^1 : F_1''(\eta) - F_0'''(\eta) = \left\{F_0''(\eta) + a\,F_0(\eta)\,F_0'(\eta) + bF_1'(\eta)\right\}c_1$$
$$\Rightarrow F_1'''(\eta) = F_0'''(\eta) + \left\{F_0''(\eta) + a\,F_0(\eta)\,F_0'(\eta) + bF_1'(\eta)\right\}c_1 \tag{25}$$

and boundary conditions are:

$$F_1(0) = 0, \ F_1'(0) = 0, F_1(1) = 0 \tag{26}$$

$$p^2 : F_2''(\eta) - F_1'''(\eta) = \left\{F_1''(\eta) + a\,F_0(\eta)\,F_1'(\eta) + a\,F_0'(\eta)\,F_1(\eta) + bF_1'(\eta)\right\}c_1 + \left\{F_0''(\eta) + a\,F_0(\eta)\,F_0'(\eta) + bF_0'(\eta)\right\}c_2$$
$$\Rightarrow F_2'''(\eta) = F_1'''(\eta) + \left\{F_1''(\eta) + a\,F_0(\eta)\,F_1'(\eta) + a\,F_0'(\eta)\,F_1(\eta) + bF_1'(\eta)\right\}c_1 + \left\{F_0''(\eta) + a\,F_0(\eta)\,F_0'(\eta) + bF_0'(\eta)\right\}c_2 \tag{27}$$

and boundary conditions are:

$$F_2(0) = 0, \ F_2'(0) = 0, F_2(1) = 0 \tag{28}$$

$$p^3 : F_3''(\eta) - F_2'''(\eta) = \left\{F_2''(\eta) + a\,F_0(\eta)\,F_2'(\eta) + a\,F_1(\eta)F_1'(\eta) + aF_0'(\eta)F_2(\eta) + bF_2'(\eta)\right\}c_1$$
$$+ \left\{F_1''(\eta) + a\,F_0(\eta)\,F_1'(\eta) + aF_0'(\eta)F_1(\eta) + bF_1'(\eta)\right\}c_2$$
$$+ \left\{F_0''(\eta) + a\,F_0(\eta)\,F_0'(\eta) + bF_0'(\eta)\right\}c_3$$
$$\Rightarrow F_3'''(\eta) = F_2'''(\eta) + \left\{F_2''(\eta) + a\,F_0(\eta)\,F_2'(\eta) + a\,F_1(\eta)F_1'(\eta) + aF_0'(\eta)F_2(\eta) + bF_2'(\eta)\right\}c_1 \tag{29}$$
$$+ \left\{F_1''(\eta) + a\,F_0(\eta)\,F_1'(\eta) + aF_0'(\eta)F_1(\eta) + bF_1'(\eta)\right\}c_2$$
$$+ \left\{F_0''(\eta) + a\,F_0(\eta)\,F_0'(\eta) + bF_0'(\eta)\right\}c_3$$

with boundary conditions as:

$$F_3(0) = 0, \ F_3'(0) = 0, F_3(1) = 0 \tag{30}$$

and so on. Solving Eq. (23) with the boundary conditions (24), we may get:

$$F_0 = 1 - \eta^2 \tag{31}$$

Again from eq. (25) with boundary conditions (26) we will obtain:

$$F_1 = \left\{\frac{a\,\eta^6}{60} - \frac{(a+b)\eta^2}{12} + \left(\frac{a}{15} + \frac{b}{12}\right)\eta^2\right\}c_1 \tag{32}$$

Further from eq. (27) and boundary conditions (28), it may be found that:

$$F_2 = \frac{-a^2 c_1^2}{5400}\eta^{10} + \frac{(a^2 + ab)c_1^2}{560}\eta^8 + \left\{\left(\frac{-a^2}{200} - \frac{ab}{120} + \frac{a}{60} - \frac{b}{360}\right)c_1^2 + \frac{(c_1 + c_2)a}{60}\right\}\eta^6$$
$$+ \left\{\left(\frac{a^2}{180} + \frac{b^2}{144} + \frac{ab}{80} - \frac{a}{12} - \frac{b}{12}\right)c_1^2 - \frac{(a+b)(c_1 + c_2)}{12}\right\}\eta^4 \tag{33}$$
$$- \left\{\left(\frac{163a^2}{75600} + \frac{b^2}{240} + \frac{ab}{168} - \frac{a}{15} - \frac{b}{12}\right)c_1^2 - \frac{(c_1 + c_2)a}{15} - \frac{bc_2}{12}\right\}\eta^2.$$

By proceeding like this we may get the functions $F_n(c_1, c_2, c_3, \ldots, c_n)$. The nth order approximate solution of Eq. (20) may be obtained as:

$$F = F_0(\eta) + F_1(\eta; c_1) + F_2(\eta; c_1, c_2) + F_3(\eta; c_1, c_2, c_3) + \ldots + F_n(c_1, c_2, c_3, \ldots, c_n) \tag{34}$$

Further as discussed in the previous section, the least-square technique may be used to find convergence controller parameter c_1 in 1st order of approximation, c_2 in 2nd order of approximation, c_3 in the 3rd order of approximation and so on. The procedure is now discussed below by taking particular values of the parameters involved in the governing differential equation.

5. Results and Discussions

Let us consider $Re = 50, \alpha = 5^0, \phi = 0, Ha = 0$. In order to compute values of unknown convergence controller parameters $c_1, c_2, c_3, \ldots, c_n$, firstly consider 1st order approximation to compute c_1 that is:

$$F = 1 - \eta^2 + \left\{ \frac{a\eta^6}{60} - \frac{(a+b)\eta^2}{12} + \left(\frac{a}{15} + \frac{b}{12} \right) \eta^2 \right\} c_1 \tag{35}$$

Here the residual error function R_1 may be obtained as:

$$
\begin{aligned}
R_1 = a &\left[2\eta + \frac{c_1(5a + 5b - a\eta^2)\eta^3}{15} - \frac{c_1(4a + 5b)\eta}{30} - \frac{ac_1\eta^5}{30} \right] \cdot \left[\eta^2 + \frac{c_1(5a + 5b - a\eta^2)\eta^4}{60} - \frac{c_1(4a + 5b)\eta^2}{60} - 1 \right] \\
&- \frac{2c_1(5a + 5b - a\eta^2)\eta}{5} - b \left[2\eta + \frac{c_1(5a + 5b - a\eta^2)\eta^3}{15} - \frac{c_1(4a + 5b)\eta}{30} - \frac{ac_1\eta^5}{30} \right] + \frac{8ac_1\eta^3}{5}.
\end{aligned}
\tag{36}
$$

Substituting eq. (36) in eq. (17) and solving the obtained algebraic equation for c_1, we may get the value of c_1 as $c_1 = -0.914259839666614$. In order to compute c_2, let us consider 2nd order approximation as:

$$
\begin{aligned}
F = 1 - \eta^2 &+ \left\{ \frac{a\eta^6}{60} - \frac{(a+b)\eta^2}{12} + \left(\frac{a}{15} + \frac{b}{12} \right) \eta^2 \right\} c_1 \\
&- \frac{a^2 c_1^2}{5400} \eta^{10} + \frac{(a^2 + ab)c_1^2}{560} \eta^8 + \left\{ \left(\frac{-a^2}{200} - \frac{ab}{120} + \frac{a}{60} - \frac{b}{360} \right) c_1^2 + \frac{(c_1 + c_2)a}{60} \right\} \eta^6 \\
&+ \left\{ \left(\frac{a^2}{180} + \frac{b^2}{144} + \frac{ab}{80} - \frac{a}{12} - \frac{b}{12} \right) c_1^2 - \frac{(a+b)(c_1 + c_2)}{12} \right\} \eta^4 \\
&- \left\{ \left(\frac{163a^2}{75600} + \frac{b^2}{240} + \frac{ab}{168} - \frac{a}{15} - \frac{b}{12} \right) c_1^2 - \frac{(c_1 + c_2)a}{15} - \frac{bc_2}{12} \right\} \eta^2
\end{aligned}
\tag{37}
$$

where $c_1 = -0.914259839666614$. Hence in this step, we have only one unknown parameter c_2. By finding the residual error function R_2 and solving the algebraic equation obtained from eq. (18) we may get $c_2 = 0.024720757858145$. By proceeding like this we may get values of convergence controller parameters as:

$$
\begin{aligned}
&c_3 = 0.004491893350062, c_4 = 0.000855995207881, c_5 = 0.000185539579073, \\
&c_6 = 0.000043477431212, c_7 = 0.000010412129498, c_8 = 0.000002447979037.
\end{aligned}
\tag{38}
$$

Finally by plugging the values of these convergence controller parameters in eq. (34), we may get the approximate solution of Eq. (20). In Table 2, we have presented obtained numerical results of non-dimensional velocity when $Re = 50, \alpha = 5^0, \phi = 0, Ha = 0$. For a convergent channel that is taking $\alpha < 0$, Table 3 consists of the velocity profile when $Re = 80, \alpha = -5^0, \phi = 0, Ha = 0$. From both these Tables 2 and 3, it may be seen that for both divergent and convergent channel we are getting convergent results by using the proposed method. Figures 2 and 3 depict the residual errors for divergent and convergent channels respectively at different orders of approximation. It is clear from these figures that with an increase in the number of terms in the series solution, the residual error decreases rapidly and moreover it tends to zero. This shows the accuracy of the proposed method. For the support of present results, Figs. 4 and 5 represent comparison graphs of obtained results with the numerical results given in Moradi et al [10] by the Runge-Kutta scheme. From these figures, we may confirm that the obtained results maintain a very good agreement with the previous results.
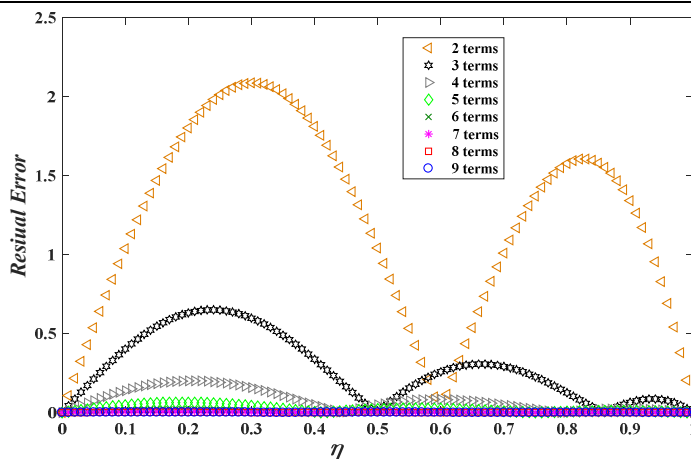
Fig. 2. Residual error at different numbers of terms in series solution when $Re = 50, \alpha = 5^0, \phi = 0, Ha = 0$.
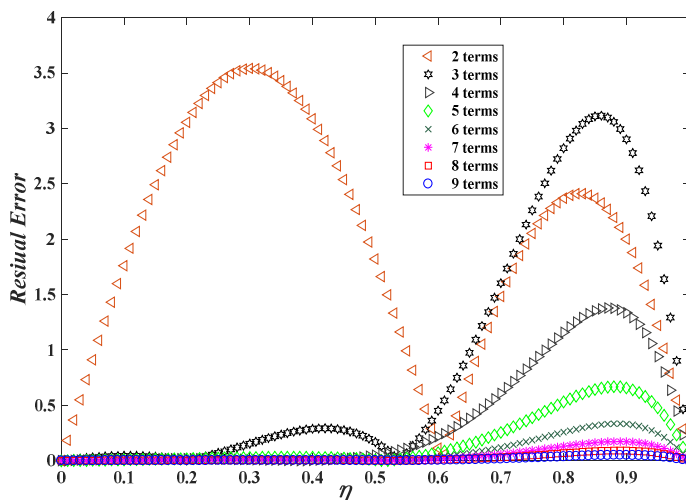

Fig. 3. Residual error at different numbers of terms in series solution when $Re = 80, \alpha = -5^0, \phi = 0, Ha = 0$.
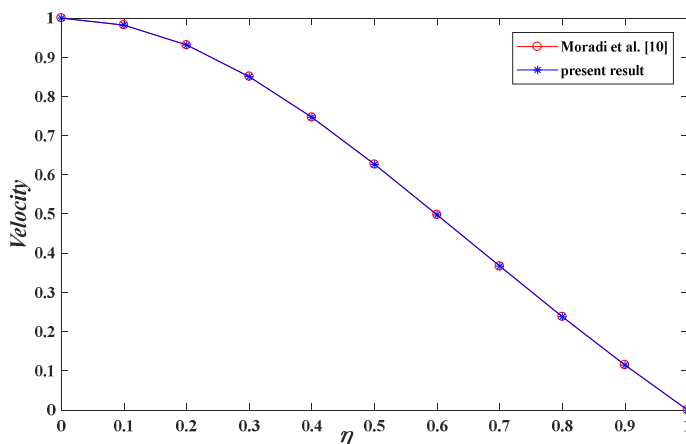

Fig. 4. Comparision between present result for divergent channel and existing result where $Re = 50, \alpha = 5^0, \varphi = \phi, Ha = 0$.

Impacts of different parameters viz. Reynolds number, Hartmann number and volume fraction on non-dimensional velocity profile have been investigated graphically. Here copper-water nanofluid has been taken into consideration to observe the impacts of these parameters. In Fig. 6 we have shown velocity values for different Reynolds number and fixed values of Ha, ϕ and α. From this figure, it may be confirmed that the velocity profile for copper-water nanofluid decreases with an increase in the Reynolds number. To show the effect of the magnetic field, velocity profiles for different values of Hartmann number and fixed values of Re, ϕ and α have been presented in Fig. 7. It may be seen from this figure that the velocity profile has increasing nature with an increase in the Hartmann number. From Fig. 8 we may observe the effect of volume fraction on the velocity profile. It may be confirmed from this figure that velocity decreases with an increase in volume fraction.
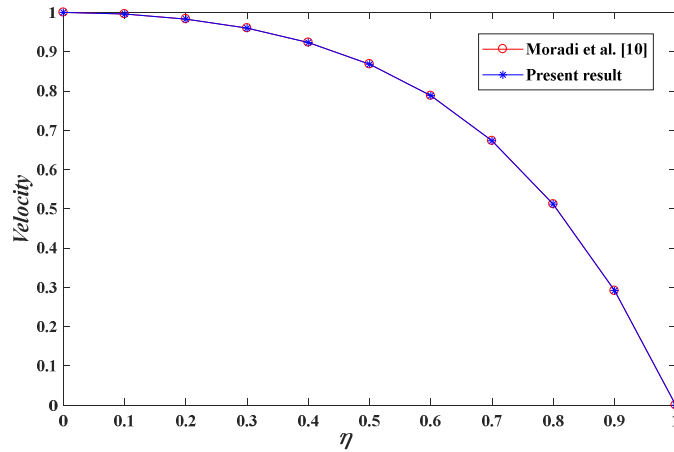
Fig. 5. Comparision between present result for convergent channel and existing result where $Re = 80, \alpha = -5^0, \phi = 0, Ha = 0$.
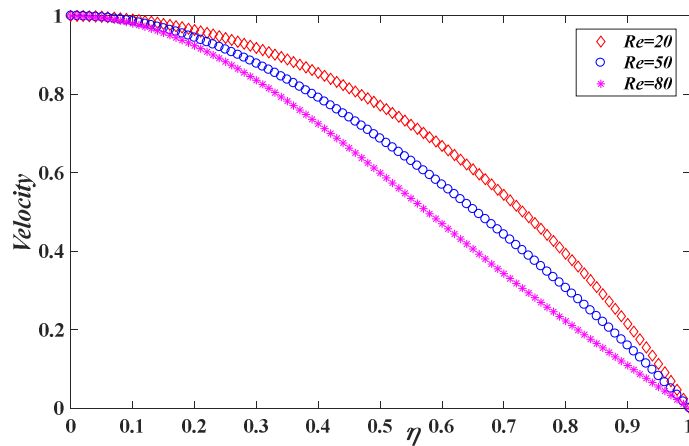

Fig. 6. Effect of Re on velocity profile for copper-water nanofluid when $\alpha = 5^0, \phi = 0.1, Ha = 30$.

Table 2. Non-dimensional velocity profile for different orders of approximation when $Re = 50, \alpha = 5^0, \phi = 0, Ha = 0$.

η	Velocity profile for different order of approximation							
	1st	2nd	3rd	4th	5th	6th	7th	8th
0.0	1	1	1	1	1	1	1	1
0.1	0.98472	0.98306	0.98261	0.98248	0.98245	0.98243	0.98243	0.98243
0.2	0.93969	0.93350	0.93186	0.93141	0.93128	0.93124	0.93123	0.93122
0.3	0.86723	0.85491	0.85176	0.85094	0.85070	0.85063	0.85061	0.85061
0.4	0.77106	0.75273	0.74832	0.74721	0.74691	0.74682	0.74680	0.74679
0.5	0.65607	0.63362	0.62859	0.62738	0.62707	0.62698	0.62695	0.62695
0.6	0.52795	0.50458	0.49974	0.49862	0.49834	0.49826	0.49824	0.49823
0.7	0.39278	0.37216	0.36817	0.36727	0.36704	0.36698	0.36697	0.36696
0.8	0.25652	0.24171	0.23895	0.23833	0.23818	0.23813	0.23812	0.23812
0.9	0.12436	0.11698	0.11558	0.11526	0.11518	0.11516	0.11515	0.11515
1.0	0	0	0	0	0	0	0	0

Table 3. Non-dimensional velocity profile for different orders of approximation when $Re = 80, \alpha = -5^0, \phi = 0, Ha = 0$.

| η	Velocity profile for different order of approximation							
	1st	2nd	3rd	4th	5th	6th	7th	8th
0.0	1	1	1	1	1	1	1	1
0.1	0.99679	0.99589	0.99595	0.99595	0.99596	0.99596	0.99596	0.99596
0.2	0.98615	0.98303	0.98324	0.98324	0.98326	0.98326	0.98327	0.98327
0.3	0.96508	0.95968	0.96005	0.96008	0.96013	0.96015	0.96016	0.96017
0.4	0.92876	0.92261	0.92317	0.92331	0.92342	0.92346	0.92349	0.92350
0.5	0.87092	0.86674	0.86770	0.86806	0.86826	0.86835	0.86840	0.86842
0.6	0.78421	0.78491	0.78669	0.78740	0.78774	0.78791	0.78799	0.78804
0.7	0.66081	0.66787	0.67089	0.67207	0.67261	0.67287	0.67300	0.67306
0.8	0.49309	0.50493	0.50902	0.51060	0.51131	0.51164	0.51180	0.51189
0.9	0.27438	0.28522	0.28889	0.29032	0.29095	0.29125	0.29140	0.29147
1.0	0	0	0	0	0	0	0	0
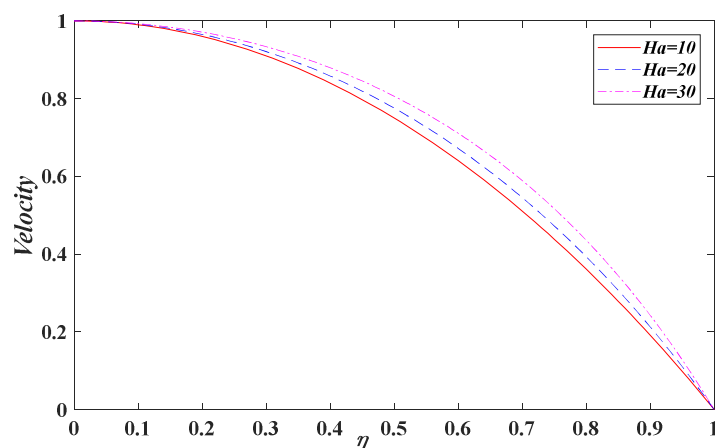
Fig. 7. Effect of Ha on velocity profile for copper-water nanofluid when $Re = 5, \alpha = 5^0, \phi = 0.1$.
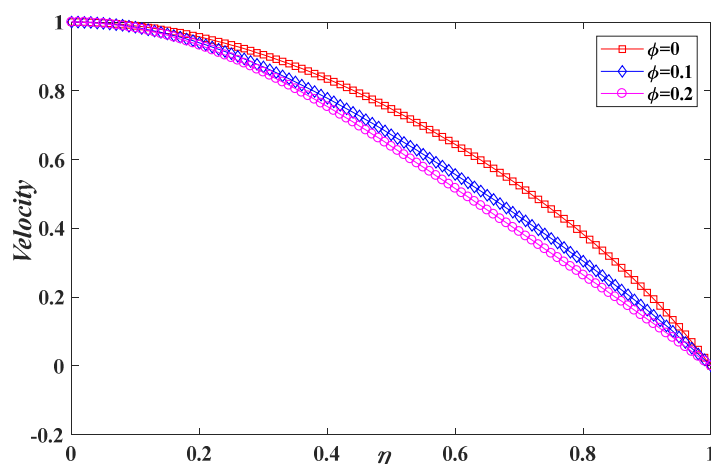

Fig. 8. Effect of ϕ on the velocity profile for copper-water nanofluid when $Ha = 50, Re = 80, \alpha = 5^0$.

6. Conclusion

The nanofluid flow between two inclined planes under the influence of the magnetic field was investigated successfully. OHAM was used to get series solution of the velocity profile. Optimal values of the convergence controller parameters used in OHAM were determined one by one with the help of the least square approximation technique. For the accuracy of the proposed method, present results were compared with existing results for some special cases viz. for fixed values of involved parameters and they were in good agreement. Moreover, the residual error tends to zero by increasing the number of terms in the series solution. For copper-water nanofluid, it was observed that velocity decreases with an increase in Reynolds number whereas velocity increases with an increase in the Hartmann number. It was also seen that the velocity profile has decreasing nature with an increase in the volume fraction.

Author Contributions

All authors have equal contribution in all sections of the manuscript.

Conflict of Interest

The authors declared no potential conflicts of interest with respect to the research, authorship, and publication of this article.

Data Availability Statements

The datasets generated and/or analyzed during the current study are available from the corresponding author on reasonable request.

Nomenclature

r	Radial coordinate	θ	Angular coordinate
v	Radial velocity	α	Angle between plates
P	Pressure	ρ	Density
B_0	Electromagnetic Induction	μ	Dynamic viscosity
F	Dimensionless velocity	σ	Conductivity
ϕ	Nanoparticle volume fraction	η	Dimensionless degree
Ha	Hartmann number	Re	Reynolds number

Subscript

nf	nanofluid
f	fluid
s	solid

References

[1] Choi, S.U.S., Enhancing conductivity of fluids with nanoparticles, *ASME Fluid Eng. Division*, 231, 1995,99-105.

[2] Rajagopal, K.R. and Na, T.Y., Natural convection flow of a non-Newtonian fluid between two vertical flat plates. *Acta Mechanica*, 54(3-4), 1985, 239-246.

[3] Kargar, A. and Akbarzade, M., Analytic solution of natural convection flow of a non-newtonian fluid between two vertical flat plates using homotopy perturbation method (HPM). *World Applied Sciences Journal*, 20(11), 2012, 1459-1465.

[4] Ziabakhsh, Z. and Domairry, G., Analytic solution of natural convection flow of a non-Newtonian fluid between two vertical flat plates using homotopy analysis method. *Communications in Nonlinear Science and Numerical Simulation*, 14(5), 2009, 1868-1880.

[5] Biswal, U., Chakraverty, S. and Ojha, B.K., Natural convection of non-Newtonian nanofluid flow between two vertical parallel plates. *International Journal of Numerical Methods for Heat & Fluid Flow*, 29(6), 2019, 1984-2008.

[6] Jeffery, G.B., L. The two-dimensional steady motion of a viscous fluid. *The London, Edinburgh, and Dublin Philosophical Magazine and Journal of Science*, 29(172), 1915, 455-465.

[7] Hamel, G., Spiralförmige Bewegungen zäher Flüssigkeiten. *Jahresbericht der deutschen mathematiker-vereinigung*, 25, 1917, 34-60.

[8] Esmaili, Q., Ramiar, A., Alizadeh, E. and Ganji, D.D., An approximation of the analytical solution of the Jeffery–Hamel flow by decomposition method. *Physics Letters A*, 372(19), 2008, 3434-3439.

[9] Sheikholeslami, M., Ganji, D.D., Ashorynejad, H.R. and Rokni, H.B., Analytical investigation of Jeffery-Hamel flow with high magnetic field and nanoparticle by Adomian decomposition method. *Applied Mathematics and Mechanics*, 33(1), 2012, 25-36.

[10] Moradi, A., Alsaedi, A. and Hayat, T., Investigation of nanoparticles effect on the Jeffery–Hamel flow. *Arabian Journal for Science and Engineering*, 38(10), 2013, 2845-2853.

[11] Umavathi, J.C. and Shekar, M., Effect of MHD on Jeffery-Hamel flow in nanofluids by differential transform method. *Int. Journal of Engineering Research and Applications*, 3(5), 2013, 953-962.

[12] Moghimi, S.M., Domairry, G., Soleimani, S., Ghasemi, E. and Bararnia, H., Application of homotopy analysis method to solve MHD Jeffery–Hamel flows in non-parallel walls. *Advances in Engineering Software*, 42(3), 2011, 108-113.

[13] Nourazar, S.S., Nazari-Golshan, A. and Soleymanpour, F., On the expedient solution of the magneto-hydrodynamic Jeffery-Hamel flow of Casson fluid. *Scientific Reports*, 8(1), 2018, 16358.

[14] Turkyilmazoglu, M., Extending the traditional Jeffery-Hamel flow to stretchable convergent/divergent channels. *Computers & Fluids*, 100, 2014, 196-203.

[15] Freidoonimehr, N. and Rashidi, M.M., Dual solutions for MHD Jeffery-Hamel nano-fluid flow in non-parallel walls using predictor homotopy analysis method. *Journal of Applied Fluid Mechanics*, 8(4), 2015, 911-919.

[16] Makinde, O.D. and Mhone, P.Y., Hermite–Padé approximation approach to MHD Jeffery–Hamel flows. *Applied Mathematics and Computation*, 181(2), 2006, 966-972.

[17] Imani, A.A., Rostamian, Y., Ganji, D.D. and Rokni, H.B., Analytical investigation of Jeffery-Hamel flow with high magnetic field and nanoparticle by rvim, *International Journal of Engineering*, 25(3), 2012, 249-256.

[18] Motsa, S.S., Sibanda, P., Awad, F.G. and Shateyi, S., A new spectral-homotopy analysis method for the MHD Jeffery–Hamel problem. *Computers & Fluids*, 39(7), 2010, 1219-1225.

[19] Farooq, U., Lu, D., Munir, S., Ramzan, M., Suleman, M. and Hussain, S., MHD flow of Maxwell fluid with nanomaterials due to an exponentially stretching surface. *Scientific Reports*, 9(1), 2019, 7312.

[20] Turkyilmazoglu, M., Fully developed slip flow in a concentric annuli via single and dual-phase nanofluids models. *Computer Methods and Programs in Biomedicine*, 179, 2019, 104997.

[21] Turkyilmazoglu, M., Free and circular jets cooled by single-phase nanofluids. *European Journal of Mechanics-B/Fluids*, 76, 2019, 1-6.

[22] Alsabery, A.I., Chamkha, A.J., Saleh, H. and Hashim, I., Natural convection flow of a nanofluid in an inclined square enclosure partially filled with a porous medium. *Scientific Reports*, 7(1), 2017, 2357.

[23] Turkyilmazoglu, M., A note on the correspondence between certain nanofluid flows and standard fluid flows. *Journal of Heat Transfer*, 137(2), 2015, 024501.

[24] Liao, S.J., *The proposed homotopy analysis technique for the solution of nonlinear problems*, Ph.D. Thesis, Shanghai Jiao Tong University, 1992.

[25] Liao, S.J., A uniformly valid analytic solution of two-dimensional viscous flow over a semi-infinite flat plate. *Journal of Fluid Mechanics*, 385, 1999, 101-128.

[26] Liao, S.J., An explicit, totally analytic approximate solution for Blasius' viscous flow problems. *International Journal of Non-Linear Mechanics*, 34(4), 1999, 759-778.

[27] Brinkman, H.C., The viscosity of concentrated suspensions and solutions. *Journal of Chemical Physics*, 20(4), 1952, 571-571.

[28] Turkyilmazoglu, M., Single phase nanofluids in fluid mechanics and their hydrodynamic linear stability analysis. *Computer Methods and Programs in Biomedicine*, 187, 2020, 105171.

[29] Marinca, V. and Herişanu, N., Application of optimal homotopy asymptotic method for solving nonlinear equations arising in heat transfer. *International Communications in Heat and Mass Transfer*, 35(6), 2008, 710-715.

[30] Marinca, V., Herişanu, N., Bota, C. and Marinca, B., An optimal homotopy asymptotic method applied to the steady flow of a fourth-grade fluid past a porous plate. *Applied Mathematics Letters*, 22(2), 2009, 245-251.

[31] Chakraverty, S., Mahato, N., Karunakar, P. and Rao, T.D., *Advanced Numerical and Semi-Analytical Methods for Differential Equations*. John Wiley & Sons, USA, 2019.

[32] Gerald, C.F., *Applied Numerical Analysis*, Pearson Education India, Bengaluru, 2004.

ORCID iD

U. Biswal https://orcid.org/0000-0003-4953-3177
S. Chakraverty https://orcid.org/0000-0003-4857-644X

How to cite this article: Biswal U., Chakraverty S. Investigation of Jeffery-Hamel Flow for Nanofluid in the Presence of Magnetic Field by a New Approach in the Optimal Homotopy Analysis Method, *J. Appl. Comput. Mech.*, 8(1), 2022, 48–59. https://doi.org/10.22055/JACM.2020.31909.1937

Publisher's Note Shahid Chamran University of Ahvaz remains neutral with regard to jurisdictional claims in published maps and institutional affiliations.